Title

A vertebrate adaptive radiation is assembled from an ancient and disjunct spatiotemporal landscape

Journal

Proceedings of the National Academy of Sciences of the United States of America, 118(20)

ISSN

0027-8424

Authors

Richards, Emilie J
McGirr, Joseph A
Wang, Jeremy R
et al.

Publication Date

2021-05-18

DOI

10.1073/pnas.2011811118

Peer reviewed

A vertebrate adaptive radiation is assembled from an ancient and disjunct spatiotemporal landscape

Emilie J. Richards[a,b], Joseph A. McGirr[c], Jeremy R. Wang[d], Michelle E. St. John[a,b], Jelmer W. Poelstra[e], Maria J. Solano[f], Delaney C. O'Connell[f], Bruce J. Turner[g], and Christopher H. Martin[a,b,1]

[a]Department of Integrative Biology, University of California, Berkeley, CA 94720; [b]Museum of Vertebrate Zoology, University of California, Berkeley, CA 94720; [c]Department of Environmental Toxicology, University of California, Davis, CA 95616; [d]Department of Genetics, University of North Carolina, Chapel Hill, NC 27514; [e]Molecular and Cellular Imaging Center, Ohio State University, Columbus, OH 43210; [f]Department of Biology, University of North Carolina, Chapell Hill, NC 27514; and [g]Department of Biological Sciences, Virginia Polytechnic Institute and State University, Blacksburg, VA 24601

Edited by Peter R. Grant, Princeton University, Princeton, NJ, and approved March 15, 2021 (received for review June 11, 2020)

To investigate the origins and stages of vertebrate adaptive radiation, we reconstructed the spatial and temporal histories of adaptive alleles underlying major phenotypic axes of diversification from the genomes of 202 Caribbean pupfishes. On a single Bahamian island, ancient standing variation from disjunct geographic sources was reassembled into new combinations under strong directional selection for adaptation to the novel trophic niches of scale-eating and molluscivory. We found evidence for two longstanding hypotheses of adaptive radiation: hybrid swarm origins and temporal stages of adaptation. Using a combination of population genomics, transcriptomics, and genome-wide association mapping, we demonstrate that this microendemic adaptive radiation of novel trophic specialists on San Salvador Island, Bahamas experienced twice as much adaptive introgression as generalist populations on neighboring islands and that adaptive divergence occurred in stages. First, standing regulatory variation in genes associated with feeding behavior (*prlh*, *cfap20*, and *rmi1*) were swept to fixation by selection, then standing regulatory variation in genes associated with craniofacial and muscular development (*itga5*, *ext1*, *cyp26b1*, and *galr2*) and finally the only de novo nonsynonymous substitution in an osteogenic transcription factor and oncogene (*twist1*) swept to fixation most recently. Our results demonstrate how ancient alleles maintained in distinct environmental refugia can be assembled into new adaptive combinations and provide a framework for reconstructing the spatiotemporal landscape of adaptation and speciation.

adaptive radiation | speciation | genomics | adaptation | hybridization

Adaptive radiations are fundamental to understanding the biodiversity of life. These bursts of phenotypic and ecological diversification may occur in response to ecological opportunity provided by unoccupied niche space (1, 2). However, the origins and major features of this process are still controversial. For example, ecological opportunity appears necessary but not sufficient to explain why only some lineages radiate and others do not after colonizing similar environments (3–6).

One hypothesis about the origins of adaptive radiation is that hybridization between species is necessary to trigger diversification, because lineages may be limited in their ability to respond to ecological opportunity by a lack of genetic variation (7, 8). Indeed, extensive histories of hybridization have been documented in many classic and spectacular radiations (9–13). Despite substantial evidence of adaptive introgression during radiation, no previous studies have compared adaptive introgression between closely related radiating and nonradiating lineages to distinguish introgression as necessary for radiation as predicted by the hybrid swarm hypothesis (but see ref. 14 for a comparison of genome-wide introgression).

A parallel debate centers on whether adaptive divergence proceeds in temporal stages. Hypotheses that speciation and adaptive radiation proceed in adaptive stages were previously based on the phylogenetic distribution of extant traits (15–20). For example, one model proposed three stages of vertebrate adaptive radiation: first shifts in habitat, followed by divergence in trophic morphology, and finally sexual communication signals like color (16). Similarly, the behavior-first hypothesis proposed that behavioral changes drive the evolution of other adaptive traits and promote speciation (21–24). However, existing evidence for these hypotheses comes from ancestral state reconstructions of rapidly diversifying traits that can be highly unreliable without fossil data (25–27). The timing of diversification on a phylogeny is also confounded by different rates of diversification across different trait axes (26); thus, rapidly evolving traits appear to have diverged most recently even if divergence occurred continuously in multiple traits.

Microevolutionary studies lend additional support to the idea that adaptation occurs in stages, particularly at the genetic level when the order of selection on mutations necessary to successfully adapt to a novel resource is known (28, 29). However, these studies are limited largely to adaptation in highly experimental settings (30–32) or along a single selective axis such as toxin resistance (33–35). Whether stages of adaptation occur along multiple ecological and sexual trait axes remains unknown. Recent population genomic approaches for investigating the timing of selection across multiple trait axes and identifying the sources of genetic variation in recent radiations provide a new opportunity to understand both the temporal and spatial dynamics of adaptation and speciation (13, 36–38).

Significance

Most biodiversity evolved in rapid bursts of new species, adaptations, and ecological niches. However, this process of adaptive radiation is poorly understood. We used large-scale genomic sequencing across the entire Caribbean range of pupfishes to understand why radiation in this group is restricted to a single Bahamian island. We found that twofold higher gene flow to this island brought in new combinations of ancient adaptive mutations needed for colonizing novel ecological niches of scale-eating and snail-eating. Adaptation occurred in stages: first selection on feeding behavior, then selection for trophic morphology, and finally refinement through gene coding change. We demonstrate that young, localized radiations can emerge from a vast pool of adaptive genetic variation spread across time and space.

Author contributions: E.J.R. and C.H.M. designed research; E.J.R., J.A.M., J.R.W., M.E.S.J., M.J.S., D.C.O., and C.H.M. performed research; E.J.R., J.A.M., J.R.W., J.W.P., B.J.T., and C.H.M. contributed new reagents/analytic tools; E.J.R., J.A.M., J.R.W., and J.W.P. analyzed data; and E.J.R. and C.H.M. wrote the paper.

The authors declare no competing interest.

This article is a PNAS Direct Submission.

[1]To whom correspondence may be addressed. Email: chmartin@berkeley.edu.

This article contains supporting information online at https://www.pnas.org/lookup/suppl/doi:10.1073/pnas.2011811118/-/DCSupplemental.

Published May 14, 2021.

Here, we use multiple lines of genomic, transcriptomic, and phenotypic evidence from a nascent adaptive radiation of Caribbean pupfishes to test the hypotheses that hybridization was necessary and strongly associated with adaptive radiation and that adaptive divergence occurred in stages. This sympatric radiation contains a widespread generalist algae-eating species, *Cyprinodon variegatus* (G), and two trophic specialists endemic to several hypersaline lakes on San Salvador Island (SSI), Bahamas: a molluscivore, *Cyprinodon brontotheroides* (M), with a unique nasal protrusion for oral-shelling snails (39) and a scale-eater, *Cyprinodon desquamator* (S), with twofold longer oral jaws (40) and adaptive strike kinematics for efficiently removing scales from the sides of prey fish (41). This clade exhibits classic hallmarks of adaptive radiation. First, trait diversification rates reach up to 1,400 times faster than nonradiating generalist populations on neighboring Bahamian islands in nearly identical hypersaline lake environments (5). Second, species divergence is driven by multiple fitness peaks on a surprisingly stable adaptive landscape (42–44). Third, craniofacial diversity and ecological novelty within the radiation exceeds all other cyprinodontid species

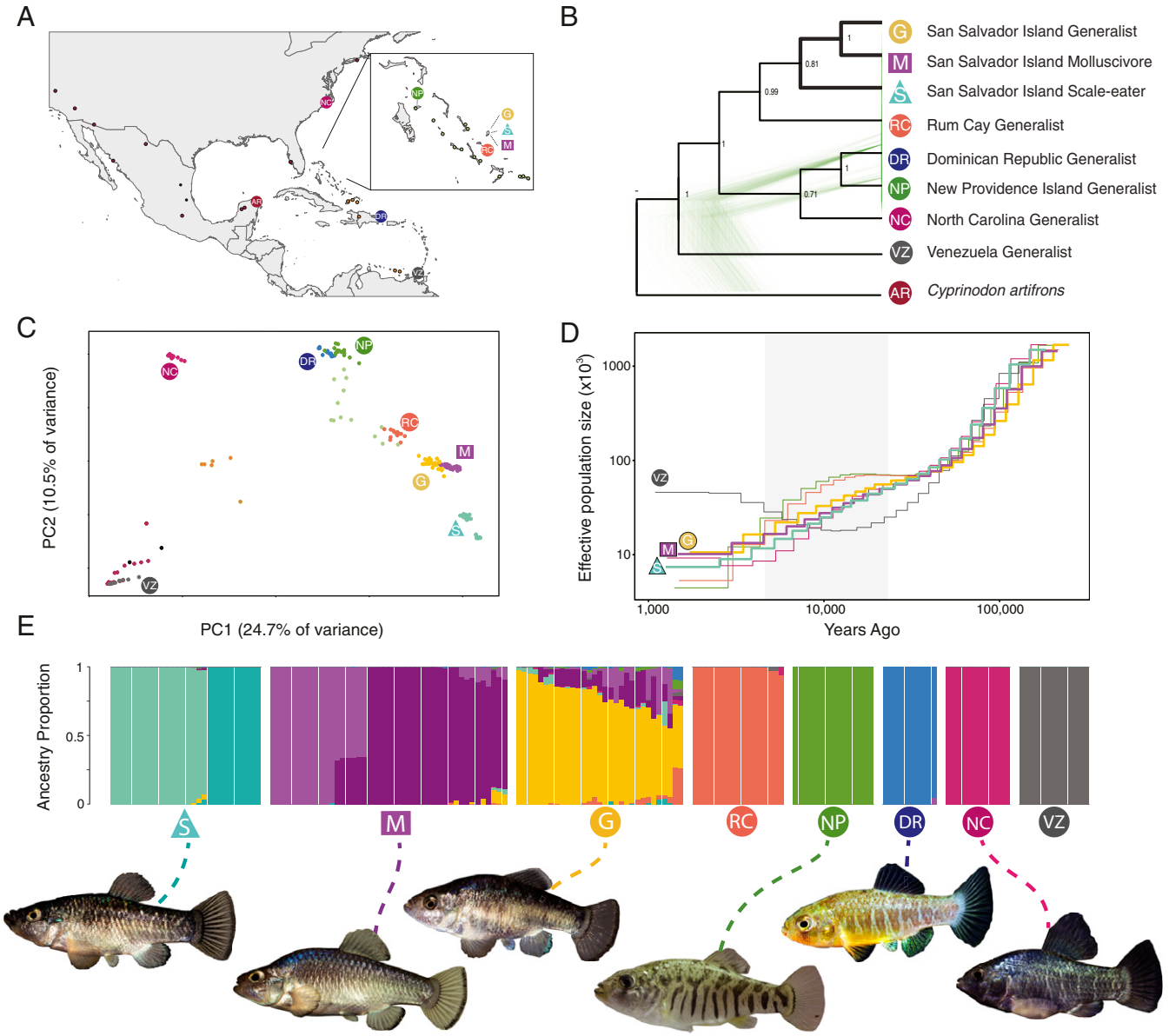

Fig. 1. Genetic diversity of pupfishes across the Caribbean. (*A*) Sample locations of *Cyprinodon* pupfishes ($n = 202$) including eight focal populations ($n \geq 10$ per population) marked with large symbols (circles: generalist populations, triangle: scale-eating pupfish, and square: molluscivore pupfish) and small dots for individuals from other locations in the Bahamas (light green), other Caribbean locations outside the Bahamas (orange), continental North and South America (maroon), and *Megupsilon* and *Cualac* outgroups to *Cyprinodon* (black). (*B*) Maximum clade credibility cladogram (black) estimated with SNAPP (48) from 10,000 SNPs for focal populations and the outgroup *Cyprinodon artifrons*. The underlying 500 gene trees (green) randomly sampled from the posterior distribution and visualized with Densitree (49) demonstrate the rapid and complex history of divergence in Caribbean pupfishes. (*C*) Principal component analysis of *Cyprinodon* pupfishes. (*D*) Changes in effective population size over time for focal populations in the Caribbean inferred using the multiple sequentially Markovian coalescent (MSMC) method (50). The gray shaded area represents the range of estimated ages for the radiation from 6 to 19 kya based on the filling of hypersaline lakes on SSI after the last glacial maximum (51–53). (*E*) Ancestry proportions across individuals on SSI (S, M, G) and five other focal Caribbean generalist populations (RC, NP, DR, NC, VZ) estimated from an LD-pruned dataset of 2.3 million SNPs in ADMIXTURE (54) with k = 11.

(5, 45). Fourth, the radiation exhibits striking divergence in other traits, including male reproductive coloration, aggressive behavior, and feeding preferences (39, 41, 46, 47).

Similar Levels of Genetic Diversity across Radiating and Nonradiating Lineages of Caribbean Pupfish

To investigate the spatiotemporal history of adaptive alleles unique to trophic specialists on SSI we constructed the first, to our knowledge, de novo hybrid assembly for *C. brontotheroides* (1.16 Gb genome size; scaffold N50 = 32 Mb; L50 = 15; 86.4% complete Actinopterygii benchmarking universal single-copy orthologs [BUSCOs]) and resequenced 202 genomes (7.9× median coverage) from across the range of *Cyprinodon* and the two closest outgroups *Megupsilon aporus* and *Cualac tessellatus* (Fig. 1*A* and *SI Appendix*, Table S1 and Dataset S1). Population structure across the Caribbean was largely explained by geographic distance (Fig. 1), and the SSI radiation did not contain higher overall genetic diversity than the rest of the Caribbean (*SI Appendix*, Fig. S1). All Caribbean populations experienced similar declines in effective population sizes following the last glacial maximum 19 kya when an order of magnitude more Caribbean coastal habitat was above sea level (Fig. 1*D*).

We scanned 5.5 million single-nucleotide polymorphisms (SNPs) across 202 Caribbean-wide pupfish genomes to identify a set of 3,258 scale-eater and 1,477 molluscivore candidate adaptive alleles, respectively. These candidate adaptive alleles showed evidence of both high genetic differentiation between trophic specialists ($F_{st} \geq 0.95$) and significant signatures of a hard selective sweep in both site frequency spectrum (SFS)–based (55) and linkage disequilibrium (LD)–based methods [(56); Fig. 2*A* and *SI Appendix*, Fig. S2 and Table S2 and Datasets S2 and S3]. We hereafter refer to these as "adaptive alleles." Overall, 45% of the selective sweeps identified in molluscivores were also identified as selective sweeps in scale-eaters but contained different fixed or nearly fixed alleles (*SI Appendix*, Fig. S3), consistent with previously observed patterns of parallel differential gene

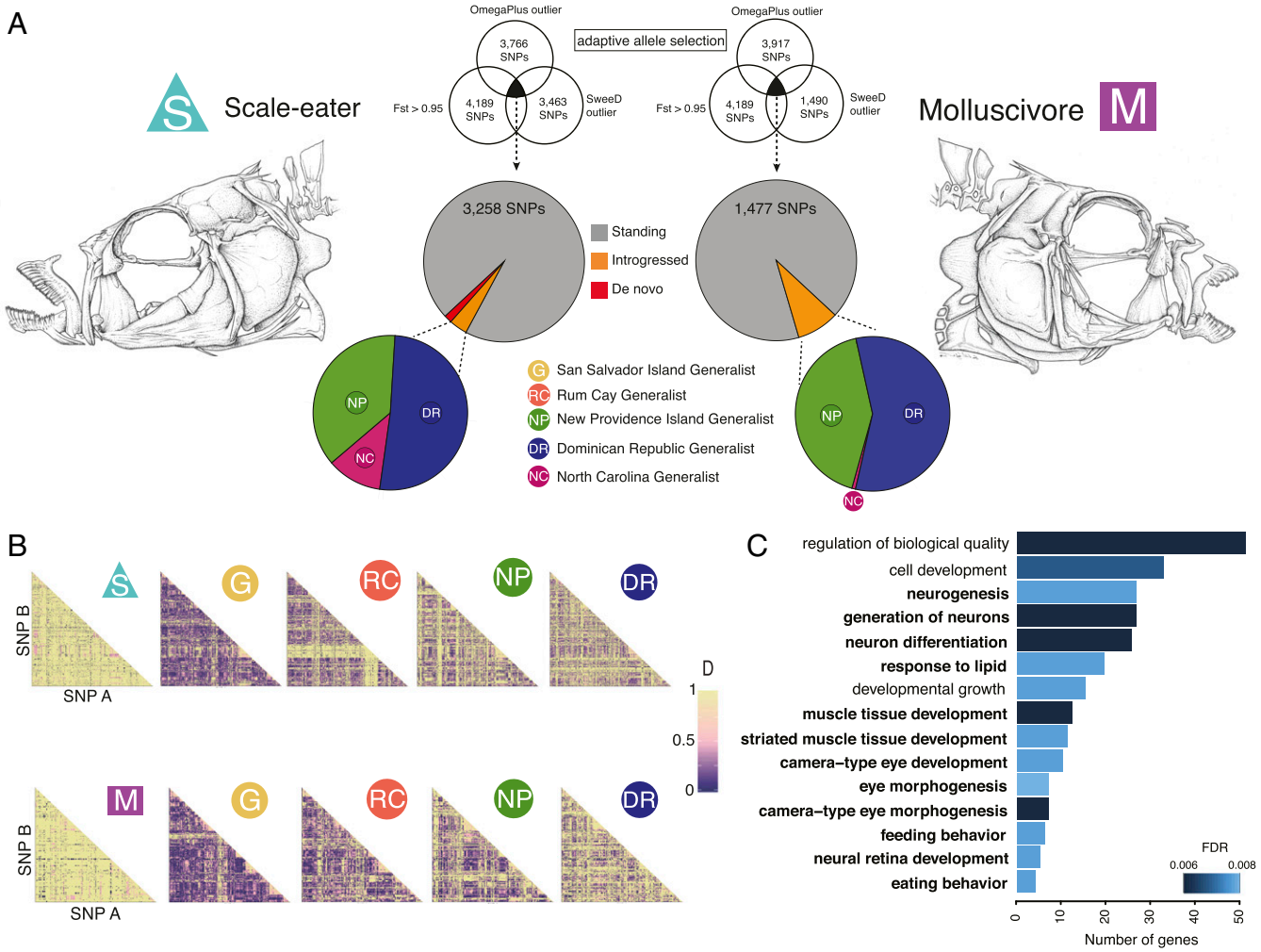

Fig. 2. All adaptive alleles differentiating trophic specialist pupfishes. (*A*) All fixed and nearly fixed adaptive alleles in each trophic specialist on SSI (filtered by $F_{st} \geq 0.95$ between specialists and evidence of a hard selective sweep from both SFS- and LD-based approaches [SweeD CLR≥ 4.47; OmegaPlus: ω >3.31]). Adaptive alleles are divided into the three major sources of genetic variation: de novo variation found on SSI only (red), introgression from a specific source population (orange), or standing genetic variation (gray). Introgressed variation is further broken down by source population: New Providence Island, Bahamas (green), Dominican Republic (blue), or North Carolina (magenta; *SI Appendix*, Tables S13–S16). (*B*) Heatmaps of linkage disequilibrium among all pairwise combinations (designated SNP A versus SNP B) of adaptive alleles for scale-eaters (S; top row) and molluscivores (M; bottom row) on SSI in comparison to linkage among these SNPs in generalists on SSI (G) and three other focal generalist populations across the Caribbean. Note the breakdown in linkage disequilibrium among adaptive alleles for trophic specialists in all generalist populations examined. (*C*) Top 15 GO categories in which scale-eater adaptive alleles were significantly enriched, with relevant terms corresponding to the major axis of trophic divergence in this radiation highlighted in bold (FDR < 0.01; full list of terms with FDR < 0.05 in *SI Appendix*, Table S5). Skull illustrations by Sean V. Edgerton.

expression in trophic specialists relative to generalists despite divergent genotypes (47).

We identified 204 genes within 20 kb of adaptive alleles (median = 1; range = 0 to 5 genes; 58% of these adaptive alleles were intergenic). Overall, 28% of adaptive alleles were found in cis-regulatory regions (within 20 kb of genes), 12% in intronic regions, and 2% in coding regions, suggesting a substantial role for gene regulatory evolution in this adaptive radiation (*SI Appendix*, Tables S3 and S4). Gene ontology (GO) enrichment analysis of adaptive alleles revealed that 12 of the top 15 most significantly enriched terms (false discovery rate [FDR] < 0.008) were related to neurogenesis, behavior, lipid metabolism, or craniofacial development, consistent with the major trophic axis of diversification in this radiation which includes foraging behavior, dietary physiology, and trophic morphology (Fig. 2*C* and *SI Appendix*, Table S5–S7). Overall, 45% of these genes were also differentially expressed between trophic specialists (FDR < 0.05; Datasets S4 and S5) in whole embryos at 2 and/or 8 days post fertilization (dpf) (47).

We then used genome-wide association mapping to identify adaptive alleles significantly associated with major axes of phenotypic diversification in the trophic specialists: caudal fin melanin pigmentation, the main axis of divergence in reproductive coloration (Fig. 1); nasal protrusion distance, a unique craniofacial feature of the molluscivore; and oral jaw size, the most divergent morphological trait of the scale-eater (>99th percentile outliers from genome-wide efficient mixed model analysis [GEMMA] posterior inclusion probabilities [PIP] while controlling for population structure on SSI: Datasets S7–S9). In total, 136 scale-eater adaptive alleles were associated with oral jaw size (20 genes), and 21 were associated with caudal fin pigmentation (three genes; Dataset S9). For the molluscivore, 152 adaptive alleles were associated with oral jaw size (6 genes), and 108 were associated with nasal protrusion distance (three genes; Datasets S7 and S8). All adaptive alleles associated with pigmentation and nasal protrusion distance were found in cis-regulatory positions within 20 kb of a gene. Overall, 89% and 99% of the adaptive alleles associated with oral jaw size in scale-eaters and molluscivores, respectively, were also cis-regulatory.

Adaptive Alleles in Trophic Specialists Are Broadly Distributed across the Caribbean but Are Only under Selection on SSI

Even though both trophic specialists are endemic to SSI, we found that nearly all their adaptive alleles occurred as standing genetic variation across the Caribbean (molluscivore: 100%; scale-eater: 98%; Fig. 2*A*). Furthermore, nearly half the adaptive alleles in SSI trophic specialists were ancient and also found in *Cualac* or *Megupsilon* outgroups to *Cyprinodon* (41% and 55% of scale-eater and molluscivore adaptive alleles, respectively), which diverged over 5 Mya from *Cyprinodon* (57). However, most adaptive alleles in SSI trophic specialists did not show any evidence of selection in other focal generalist populations (only 2% and 6% of scale-eater and molluscivore alleles, respectively; *SI Appendix*, Fig. S3), and strong linkage disequilibrium among adaptive alleles in the SSI trophic specialists was not observed in these populations (Fig. 2*B*). Thus, we conclude that trophic specialist traits within a micro-endemic adaptive radiation were almost entirely assembled from ancient standing genetic variation through strong selection for new combinations of adaptive alleles.

Stronger Signatures of Hybridization and Adaptive Introgression in Radiating Lineages

Multiple lines of evidence suggest that more hybridization and adaptive introgression took place in SSI populations than other Caribbean island populations, consistent with the hypothesis that hybridization aids adaptive radiation (Fig. 3). First, the strongest signal of introgression across the Caribbean was into the root node of the SSI radiation (Fig. 3*B*). Second, trophic specialists on SSI experienced at least twice as much adaptive introgression as other generalist populations across the Caribbean (Mann–Whitney *U* test: $P = 0.01$ and 0.03 for scale-eaters and molluscivores, respectively; *SI Appendix*, Fig. S3 *D* and *E*). Third, the distribution of tract lengths for adaptive introgression regions was narrower, and these tracts were smaller than the overall distribution of introgressed tracts, suggesting that most adaptive introgression resulted from older hybridization events, despite evidence of recent and continuous introgression to the present (Fig. 3 *E* and *F*).

Timing of Divergence and Selection Supports Temporal Stages of Adaptation

SSI pupfish diversified in their specialized foraging behavior on scales or snails, trophic morphology of their craniofacial skeleton and musculature, and in their male reproductive coloration, predominantly through contrasting melanin pigmentation throughout the fins and body (Figs. 1 and 4). We searched all genes in or near adaptive alleles for GO terms relevant to these traits, including feeding behavior, muscle and craniofacial development, and pigmentation (Ensembl 96; *SI Appendix*, Tables S5–S7). With the exception of pigmentation, these terms were all highly enriched GO categories (Fig. 2 and *SI Appendix*). We then tested for stages of adaptation across these multiple trait axes and spatial sources by estimating the relative ages of selective sweeps for all adaptive alleles in or near genes with behavioral or craniofacial annotations and all introgressed and de novo adaptive alleles. We complemented this approach with divergence time estimates between specialists calculated using a measure of absolute divergence (D_{xy}) in the regions surrounding adaptive alleles. For both approaches, time estimates were scaled by a spontaneous mutation rate per generation of 1.56×10^{-8} per base pair, estimated from high-coverage (15–69×) sequencing of two independent pedigreed crosses of SSI species and one to two F1 offspring.

Similar to patterns observed in the vertebrate stages and behavior-first hypotheses (21, 22, 24, 23), independent adaptive alleles in the cis-regulatory regions of three genes associated with feeding behavior [*prlh*, *cfap20*, and *atp8a1*; (58–62)] were the first three hard sweeps out of all adaptive alleles in our sample associated with behavior, trophic morphology, or pigmentation (Fig. 4). These adaptive alleles were much older than the radiation itself and originated as standing genetic variation in the Caribbean (Fig. 4*A*). Feeding behavior was a significantly enriched category in our GO analysis of all genes associated with adaptive alleles (FDR = 0.008; Fig. 2*C*). Mutations in the prolactin-releasing hormone gene (*prlh*), a hormone involved in stimulating milk production in mammals, also cause overeating in mice (59) and may plausibly cause different foraging preferences between SSI specialists. Concurrently, adaptive alleles in the cis-regulatory allele for cilia- and flagella-associated protein 20 (*cfap20*) were swept to fixation by selection, which affects cilia formation during brain development. *Cfap20* knockouts in *Drosophila* exhibit behavioral defects that affect foraging performance (58). *Cfap20* and *prlh* were also differentially expressed between trophic specialists in 2 and 8 dpf whole embryos respectively, consistent with adaptive alleles in the cis-regulatory regions of these genes [Datasets S4 and S5; (47)].

We observed significant "behavior-first" adaptation in which three of the five hard selective sweeps containing genes associated with feeding behavior occurred before any selective sweeps containing genes associated with craniofacial morphology (permutation test: $n = 22$, $P = 0.01$; Fig. 4*A*). This pattern was not due to local mutation rate variation and was consistent across two independent sweep age estimates and across different populations (*SI Appendix*, Figs. S11 and S13–S15). This initial stage of adaptive divergence in feeding behavior between trophic specialists suggests that behavioral changes might be crucial for initiating trophic specialization. For example, an increased drive to eat due to divergent regulation of *prlh* might be necessary to gain sufficient

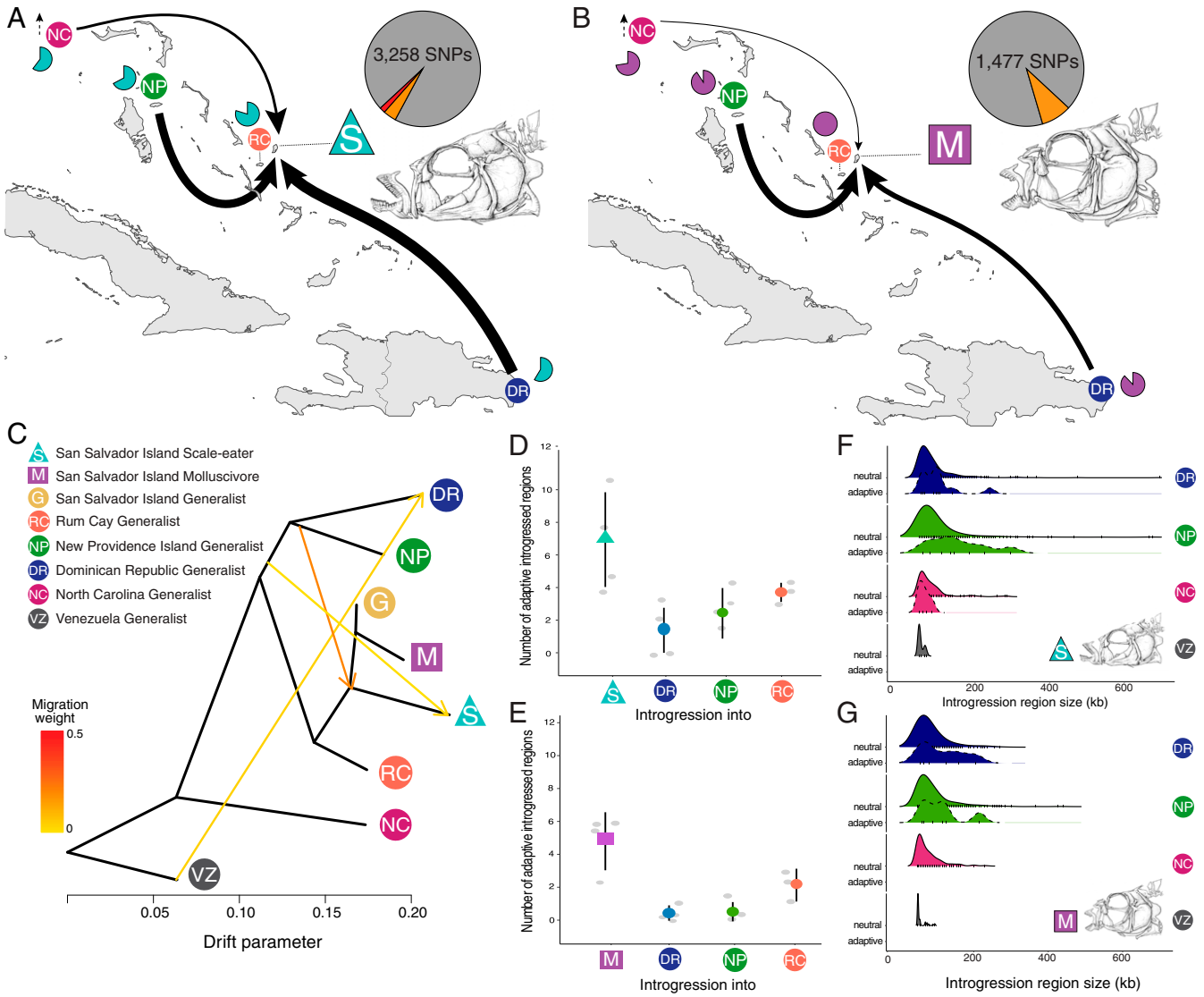

Fig. 3. History of hybridization across the Caribbean. (*A* and *B*) Summary map of adaptive introgression into SSI trophic specialists from focal generalist populations across the Caribbean. Arrow thickness is proportional to the number of adaptive introgression regions (outliers based on ms-move simulations with no migration; $f_d > 0.71$; *SI Appendix*, Table S10). Pie charts represent the percentage of all scale-eater (*A*; teal) and molluscivore (*B*; purple) adaptive alleles segregating in outgroup generalist populations across the Caribbean. (*C*) Genome-wide population graph inferred from Treemix with the three strongest signals of introgression. Note that the strongest signal (in orange) is into the root node of the SSI radiation. (*D* and *E*) Number of adaptive introgression regions in each focal population (bootstrapped mean and 95% CI in black). Gray dots represent the number of adaptive introgression regions in each focal population from each of the four source populations (*SI Appendix*, Table S12). Note that the total number of adaptive introgression regions is often larger in specialists (S, M) than in other outgroup generalist populations. (*F* and *G*) Density plots of the tract lengths of adaptive introgression regions (f_d and selective sweep outliers: dashed line) and all introgression regions (f_d outliers only: solid line). Small tick marks below density plots indicate observed introgression regions.

nutrition from eating scales (~50% of the scale-eater's diet) despite the energetic costs of high-speed strikes (40).

However, more recent sweeps of adaptive alleles near genes associated with feeding regulatory behavior in mice [*rmi*, *slc16a1*; (60, 63)] and behavior in general (*chrna7*, *nr4a2*, and *ncoa2*) indicated that adaptive divergence of behavior was not restricted entirely to this first stage. Furthermore, at least two genes associated with adaptive alleles in our dataset (*th*, *atp8a2*) have pleiotropic effects on both behavior and craniofacial morphology based on GO annotations (*SI Appendix*, Table S5–S7). The pleiotropic impacts of alleles across different trait axes and stages of adaptation are likely underestimated due to still poorly understood phenotypic effects of gene regulatory networks, particularly for the complex phenotypes of behavior and craniofacial morphology (64).

In a second stage of adaptive divergence in trophic morphology, adaptive alleles in the regulatory regions of genes associated with muscle development (*smyd1*, *kcnk2)* and craniofacial morphology (*itga5*, *tiparp*, *ext1*, *cyp26b1*, and *galr2*) swept to fixation from Caribbean-wide standing genetic variation and introgressed from three different outgroup populations across the Caribbean (Fig. 4 *E* and *F*). For example, after the initial sweep of behavioral alleles, standing genetic variation in the cis-regulatory region of the gene integrin alpha-5 (*itga5*) swept to fixation in the scale-eater (95% highest posterior density [HPD]: 639–932 ya; Fig. 4*E*). *Itga5* is involved in cranial and pharyngeal arch development in zebrafish (65, 66). Concurrently, standing variation and a de novo adaptive allele in the cis-regulatory region of the gene *galr2* swept to fixation in the scale-eater (95% HPD: 696–1,008 ya; Fig. 4*E*). *Galr2* is another strong craniofacial candidate in this system because this gene

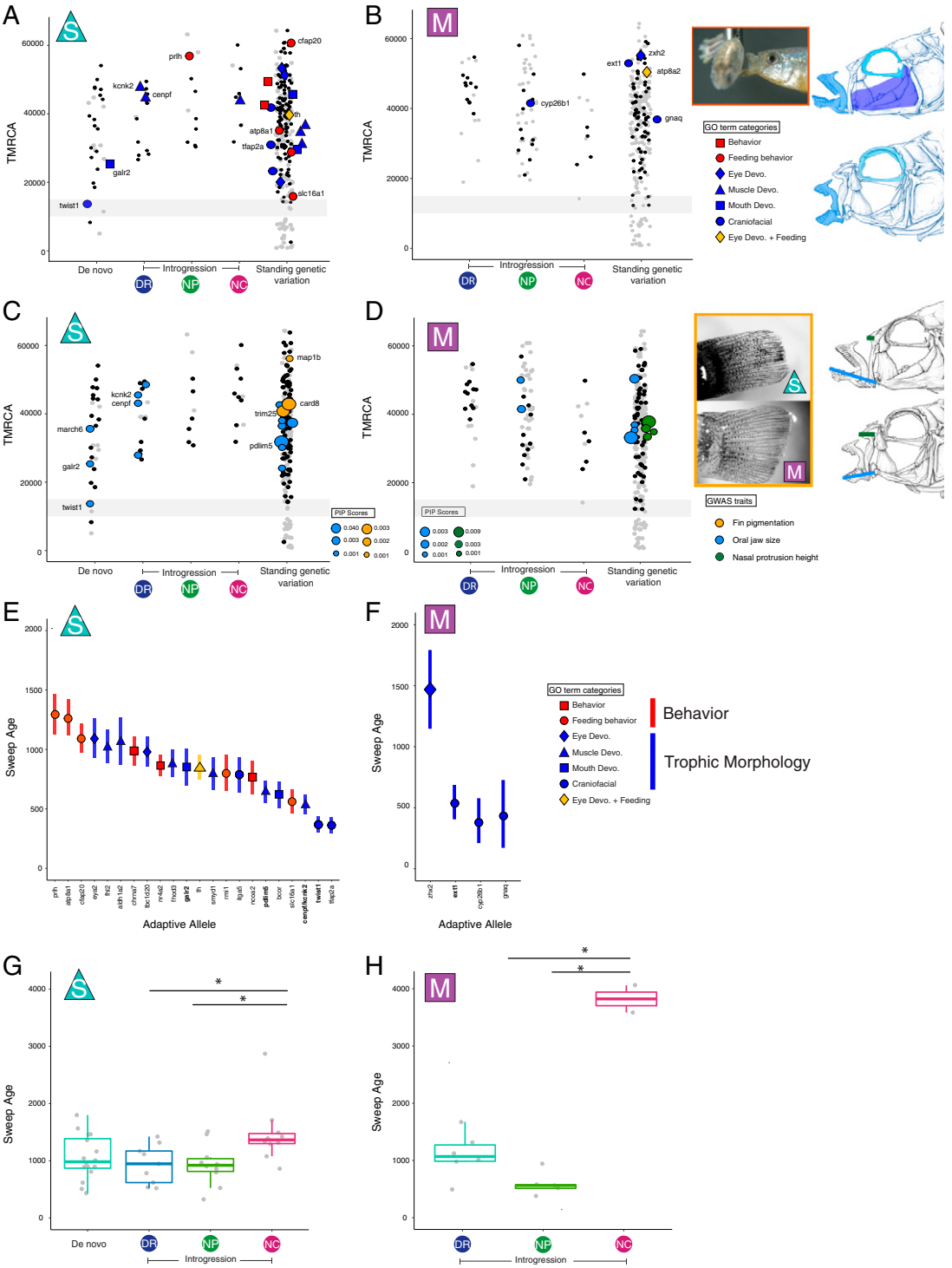

Fig. 4. The spatiotemporal landscape of adaptive radiation. (*A* and *B*) Time to most recent common ancestor (TMRCA) of adaptive alleles based on D_{xy} in the 50 kb windows containing adaptive alleles. Each column separates adaptive alleles by their spatial distribution: de novo (SSI only), adaptive introgression from one of three outgroup populations (DR: Dominican Republic, NP: New Providence, NC: North Carolina), and standing genetic variation. Gray bars highlight the approximate origins of the microendemic radiation on SSI at ~6 to 19 kya [based on geological age estimates for filling of hypersaline lakes on SSI (51, 52) since the last glacial maximum (53)]. All adaptive alleles associated with genes for behavior (red) and craniofacial morphology (blue) are illustrated by a colored point. Black points show adaptive alleles for nonfocal GO terms or unannotated; gray points show all fixed or nearly fixed alleles between specialists ($F_{st} \geq 0.95$) with no signal of a hard selective sweep; and triangles show adaptive alleles associated with pigmentation. Genes discussed in the text are labeled by their associated adaptive allele. (*C* and *D*) Adaptive alleles are colored by significant association (>99th PIP percentile GEMMA) with oral jaw size, caudal fin pigmentation, and nasal protrusion distance in scale-eaters (*C*) and molluscivores (*D*). Dot sizes scale with PIP score. (*E* and *F*) Ninety-five percent HPD intervals for selective sweep ages in the scale-eaters and molluscivores. Adaptive alleles within 20 kb of genes are colored by their GO annotations. Bolded genes were significantly associated with oral jaw size in (*E*) scale-eaters or nasal protrusion distance in (*F*) molluscivores in the GWAS analysis (>99th percentile PIP; Datasets S7–S9). (*G* and *H*) Boxplots of selective sweep ages across de novo and introgressed adaptive alleles from the three focal outgroup generalist populations. Asterisks indicate significant differences in sweep ages between different source populations (ANOVA, $P < 0.03$).

produces a transmembrane receptor for galanin, a peptide known to facilitate bone formation (67), it was significantly associated with SSI pupfish oral jaw size (99.6th PIP percentile GEMMA; Fig. 4*C* and Dataset S6), and it lies within a significant quantitative trait locus (QTL) that accounted for 15% of the variation in oral jaw size in an F2 intercross between SSI specialist species [*SI Appendix*, Table S8; (68)].

Similar to the refinement stage of adaptation proposed in the Long-Term Evolution Experiment (30), we found evidence for a final refinement stage in the radiation. We observed that two adaptive alleles associated with craniofacial morphology swept to fixation significantly more recently in the scale-eater than any other behavioral or craniofacial adaptive alleles [*tfap2a* and *twist1* (69–71); Fig. 4*E*]. Intriguingly, one of these alleles was the only nonsynonymous substitution associated with trophic morphology. This substitution occurred in the second exon of *twist1*, a transcription factor known to affect cleft palate and oral jaw size (71). Furthermore, this variant was significantly associated with SSI pupfish oral jaw size in a genome-wide association scan (99.5th PIP percentile GEMMA; Fig. 4*C*) and is highly conserved across ray-finned fishes (genome evolutionary rate profiling [GERP] score: 2.19; *SI Appendix*, Fig. S4). The second sweep that occurred at the same time as *twist1* involved adaptive alleles in the regulatory position of the gene *tfap2a*. Selection on these alleles may have occurred recently because *tfap2a* appears to be highly pleiotropic, affecting melanocyte, eye, bone, skin, and neuron development (69, 72, 73). A final stage of refinement is known from several theoretical and empirical studies of adaptive walks, in which large effect mutations are selected upon only after mutations that minimize their pleiotropic fitness costs arise and fix in the population (32, 35, 74).

We did not observe a strong initial stage of behavioral divergence in the molluscivores. Adaptive alleles for the molluscivore were found in the cis-regulatory region of only a single gene associated with feeding behavior, motor neuron, and eye development, *atp8a2* (75, 76). These adaptive alleles are among the oldest standing genetic variation, six times older than the radiation itself (Fig. 4 *B* and *D*). However, the molluscivore also experienced more recent sweeps associated with trophic morphology (Fig. 4*F*). Some of the clearest examples were four adaptive alleles in the cis-regulatory region of *ext1*, a gene that causes osteocartilaginous tumors and cranial abnormalities (77, 78), originating from Caribbean-wide standing genetic variation. These alleles were also strongly associated with nasal protrusion distance in our genome-wide association study (GWAS) (99.9th PIP percentile GEMMA; Dataset S7), and *ext1* was differentially expressed between trophic specialist whole embryos at 8 dpf (Dataset S4).

We found no evidence for a distinct stage of diversification in sexual signals, despite the striking contrast in male reproductive coloration between SSI trophic specialists in their overall melanin pigmentation exceeding all other *Cyprinodon* species (40). Instead, adaptive alleles associated with melanin pigmentation swept to fixation throughout the process of adaptive radiation. We identified adaptive cis-regulatory alleles in three genes known to affect pigmentation in model organisms [*tfap2a*, *th*, and *card8* (73, 79, 80)] and two additional adaptive alleles associated with caudal fin melanin pigmentation in SSI pupfishes (>99th PIP percentile GEMMA; Fig. 4 *C*–*E* and Dataset S7). For example, two adaptive alleles in the regulatory region of *card8* originating from standing variation swept to fixation early in the scale-eaters (95% HPD: 866–1,491 ya). This gene, which is associated with vitiligo and pigmentation loss in humans (80), was significantly associated with pupfish caudal fin pigmentation (99.2nd PIP percentile GWAS; Fig. 4*C* and Dataset S7) and was differentially expressed between trophic specialists in 2 and 8 dpf whole embryos (*SI Appendix* and Datasets S4, S5, and S7). Adaptive alleles in the cis-regulatory regions of *tfap2a* and *th* also swept to fixation in the scale-eaters more recently from standing variation (95% HPD: 292 to 431 ya and 746 to 958 ya, respectively; Fig. 4*E*). Gene knockouts of *tfap2a* cause skin pigmentation defects in mice (72, 73), and the gene *th* is associated with skin pigmentation defects in humans (79) and cuticle pigmentation defects in insects (81). This broad range of sweep ages across candidate pigmentation adaptive alleles suggests that the distinctive light/dark reproductive coloration associated with trophic specialists diverged throughout the course of adaptive radiation on SSI while repeatedly drawing from existing Caribbean-wide standing genetic variation rather than during a final stage. This is consistent with the necessary role of premating isolation for adaptation to divergent niches in sympatry (82–84).

Microendemic Radiation Was Assembled from Spatially Disjunct Pools of Adaptive Alleles

Along with temporal stages of adaptive divergence, we also found disjunct spatial patterns in the sources of adaptive introgression. Introgression from different regions of the Caribbean brought in adaptive alleles for different major axes of phenotypic diversification within the radiation. Adaptive alleles near genes annotated for feeding behavior (*prlh*; Fig. 4*A*) and oral jaw size (*cyp26b1* (85, 86); 98th PIP percentile GEMMA; Fig. 4*D* and Dataset S8) originated in the northwestern Bahamas (New Providence Island, Exumas, and Cat Island) whereas adaptive introgression of alleles near genes associated with muscle and eye development originated in the Dominican Republic (*cenpf*, *eya2*; Fig. 4*A*). Selective sweeps of adaptive alleles from different sources also occurred at largely distinct times during the radiation (Fig. 4 *G* and *H* and *SI Appendix*, Fig. S5). For example, selective sweeps of adaptive alleles from North Carolina were significantly older sweeps of introgressed variation than other populations (ANOVA, $P < 0.03$, *SI Appendix*, Fig. S4 *G* and *H*). This surprisingly disjointed spatiotemporal patchwork of adaptive introgression across the Caribbean suggests that the extant SSI radiation of trophic specialists was reassembled from distinct pools of genetic variation. Our results are consistent with at least two distinct environmental refugia in other regions of the Caribbean, perhaps due to previous ephemeral adaptive radiations, bridging micro- and macroevolutionary-scale processes (87, 88).

Microendemic Adaptive Radiations Originate over Vast Expanses of Space and Time

We conclude that hybridization substantially contributed to an adaptive radiation of trophic specialist pupfishes endemic to a single island and that the resulting adaptive divergence occurred in stages. The radiation originated from a largely ancient set of alleles maintained within different pools of standing variation in Caribbean and mainland generalist populations. Temporal stages of adaptation observed in this nascent radiation are consistent with selection on behavioral divergence first. Adaptive divergence in trophic morphology occurred next, followed by a final stage of refinement including a nonsynonymous substitution in the scale-eaters within a craniofacial transcription factor.

Additionally, our study provides a unique look at the spatial dynamics of alleles involved in adaptive divergence. We found that most adaptive alleles contributing to the major axes of ecological and sexual diversification in this radiation existed in Caribbean generalist populations long before the trophic specialist species on SSI diverged. This genetic variation is distributed across two orders of magnitude larger spatial and temporal scales than the 10 kya radiation endemic to a single 20 km island. Our results show that adaptive radiations can occupy expansive evolutionary spaces: spanning the existing radiation itself and the multitude of both past and present ephemeral pools of genetic variation that contributed to rapid diversification.

Our understanding of the origins of adaptive radiation in this system remains incomplete. The presence of adaptive introgression in both radiating and nonradiating lineages suggests hybridization was necessary but perhaps not sufficient to trigger adaptive

radiation. More subtle factors such as transient increases in lake productivity or intermediate "stepping-stone" species needed to access novel fitness peaks (9) might help explain why pupfish adaptive radiations are restricted to SSI and only one other known lake in the Caribbean (45). Our study highlights the utility and necessity of including closely related outgroups as controls in testing hypotheses about the mechanisms underlying adaptive radiation. The coincidence of hybridization, ecological opportunity, and sexual selection appear to be the best predictors of adaptive radiation in general (4, 8, 14). Most adaptive radiations, including stickleback, African cichlids, Lake Tana cyprinids, *Anolis* lizards, *Heliconius* butterflies, Hawaiian tetragnathids, and *Brocchinia* bromeliads, share similar patterns of spatial nesting within a widespread clade and intermediate levels of population structure and admixture (88, 89, 90), and we expect similar dynamics to the pupfish system. Research into the broader spatiotemporal landscape of radiations can provide insights about longstanding hypotheses of adaptive radiation and their contributions to global patterns of biodiversity.

Materials and Methods

Sampling and Population Genotyping. *Cyprinodon* pupfishes were collected from across their entire Atlantic and Caribbean range from Massachusetts to Venezuela. Individual DNA samples were resequenced using Illumina Hiseq 4000 and Novaseq. We first constructed a hybrid de novo assembly of the *C. brontotheroides* genome (1.16 Gb genome size; scaffold N50 = 32 Mb; details in *SI Appendix*). All reads were aligned to this assembly, and variants were called and filtered following the best practices guide recommended in the Genome Analysis Toolkit (91). The final dataset used in downstream analyses included 5.5 million SNPs from 202 individuals sampled from 39 localities. This included population level sampling ($n > 8$ individuals) for the three SSI species and five generalist outgroup populations (Fig. 1*A*). To visualize population structure and admixture among Caribbean populations in our dataset, we ran a principal component analysis using the eigenvectors from plink's pca function [v.1.9 (92)] and estimated the proportion of shared ancestry among individuals using ADMIXTURE [v.1.3.0 (54)] on an LD-pruned subset of 2.6 million alleles (*SI Appendix*).

Classification of Adaptive Alleles in the SSI Radiation. We first identified fixed or nearly fixed alleles ($F_{st} \geq 0.95$ between specialists: 4,189) that also showed significant evidence of a hard selective sweep in either specialist population using both SFS-based and LD-based methods SweeD and OmegaPlus (significance thresholds based on neutral simulations with ms-move: composite likelihood ratio [CLR] > 4.47 and $\omega > 3.31$; Fig. 2*A* and *SI Appendix*, Tables S2–S4 and S10). We then characterized the potential function of these adaptive alleles in the specialists in three ways. First, we performed GO enrichment analyses for genes within 20 kb of adaptive alleles using ShinyGo (93). Additionally, we looked for overlap between genes associated with adaptive alleles and genes previously found to be differentially expressed between the two specialists in whole embryos at 2 and 8 dpf (47). Lastly, we employed a Bayesian sparse linear mixed model implemented in the software package GEMMA (94) to identify genomic regions associated with variation in lower oral jaw length, caudal fin pigmentation, and nasal protrusion distance across all 78 wild-collected samples of the three SSI species (*SI Appendix*).

Characterizing Introgression and Spatial Distributions of Adaptive Alleles across the Caribbean. We identified introgression in the specialists in the SSI radiation and generalist outgroup populations on both a genome-wide and local level using Treemix (95) and the f_d statistic [(96); Fig. 3]. For both specialists, we then looked for introgressed regions that also showed evidence of a hard selective sweep to characterize candidate adaptive introgression regions. For comparison, we searched for similar signatures of adaptive introgression in three Caribbean outgroup generalist populations (excluding North Carolina and Venezuela due to lack of equivalent set of outgroup taxa for a four-population test of introgression; *SI Appendix*, Table S12).

We surveyed all pupfish populations in our dataset for the scale-eater and molluscivore adaptive alleles. These adaptive alleles were separated into three categories: de novo (observed only on SSI), standing genetic variation (observed in at least one generalist population outside of SSI), or introgressed (outlier f_d tests for introgression, significance-based on no-migration simulations with ms-move; $f_d > 0.72$; *SI Appendix*, Tables S11–S16). Introgressed adaptive alleles were further separated by geographic source (Fort Fisher, North Carolina; Lake Cunningham, New Providence Island, Bahamas; or Laguna Bavaro, Dominican Republic).

Detection of Stages of Adaptation through Divergence Times and Timing of Selective Sweeps. For all fixed or nearly fixed alleles, we estimated the timing of divergence in the 50 kb region surrounding the variant based on the amount of genetic variation that accumulated between the two specialists. All time estimates were converted to years using a pupfish generation time of 1 year (5) and a spontaneous mutation rate (1.56×10^{-8}) based on two independent sets of pedigree crosses of SSI pupfishes (*SI Appendix*, Table S9).

We estimated the age of the selective sweeps for all adaptive alleles near or within genes annotated for behavior or trophic morphology GO terms (eye, musculature, mouth, or craniofacial development) from our GO enrichment analyses using coalescent approaches implemented in starTMRCA (time to most recent common ancestor) and McSwan [(38, 97); *SI Appendix*, Table S17–S19]. We also estimated sweep ages for the entire set of de novo and introgressed adaptive alleles. We then compared the 95% HPD intervals of age estimates to visualize temporal stages of adaptation across different spatial sources of genetic variation.

Data Availability. Genomic and RNA sequence data are archived at the National Center for Biotechnology Information (NCBI) Sequence Read Archive BioProject Database (PRJNA690558; PRJNA394148, PRJNA391309; and PRJNA305422) (98–101), the *C. brontotheroides* reference genome is archived at the Whole Genome Sequences BioProject Database (PRJNA685538) (102), and additional data and scripts are on the Dryad Digital Repository https://doi.org/10.6078/D1C12S (103) and Github (https://github.com/joemcgirr/fishfASE and https://github.com/emiliejrichards/Spatiotemporal-Landscape-Caribbean-Pupfish) (104, 105).

ACKNOWLEDGMENTS. We thank Rebecca Tarvin and four anonymous reviewers for helpful comments on the manuscript; the Gerace Research Centre and Troy Day for logistical support; the governments of the Bahamas, Dominican Republic, and Venezuela, NC Wildlife Resources Commission, US National Park Service, and US Fish and Wildlife Service for permission to collect and export samples; the Zoological Society of London's Fish Net program and Dallas Children's Aquarium for additional samples; the Vincent J. Coates Genomics Sequencing Center and Functional Genomics Laboratory at the University of California, Berkeley for performing whole-genome library preparation and sequencing (supported by NIH S10 OD018174 Instrumentation Grant); and the University of California, Berkeley and University of North Carolina at Chapel Hill for computational resources. This research was funded by the NSF Division of Environmental Biology (DEB) CAREER grant 1749764, NIH grant 5R01DE027052-02, the University of North Carolina at Chapel Hill, and the University of California, Berkeley to C.H.M. and graduate research funding from the Museum of Vertebrate Zoology to E.J.R.

1. G. G. Simpson, *Tempo and Mode of Evolution* (Columbia University Press, ed. 15, 1944).
2. J. T. Stroud, J. B. Losos, Ecological opportunity and adaptive radiation. *Annu. Rev. Ecol. Evol. Syst.* **47**, 507–532 (2016).
3. D. H. Erwin, Novelty and innovation in the history of life. *Curr. Biol.* **25**, R930–R940 (2015).
4. C. E. Wagner, L. J. Harmon, O. Seehausen, Ecological opportunity and sexual selection together predict adaptive radiation. *Nature* **487**, 366–369 (2012).
5. C. H. Martin, The cryptic origins of evolutionary novelty: 1000-fold faster trophic diversification rates without increased ecological opportunity or hybrid swarm. *Evolution* **70**, 2504–2519 (2016).
6. D. L. Rabosky, Diversity-dependence, ecological speciation, and the role of competition in macroevolution. *Annu. Rev. Ecol. Evol. Syst.* **44**, 481–502 (2013).
7. O. Seehausen, Hybridization and adaptive radiation. *Trends Ecol. Evol.* **19**, 198–207 (2004).
8. D. A. Marques, J. I. Meier, O. Seehausen, A combinatorial view on speciation and adaptive radiation. *Trends Ecol. Evol.* **34**, 531–544 (2019).
9. E. J. Richards, C. H. Martin, Adaptive introgression from distant Caribbean islands contributed to the diversification of a microendemic adaptive radiation of trophic specialist pupfishes. *PLoS Genet.* **13**, e1006919 (2017).
10. J. I. Meier *et al.*, Ancient hybridization fuels rapid cichlid fish adaptive radiations. *Nat. Commun.* **8**, 14363 (2017).
11. The Heliconius Genome Consortium, Butterfly genome reveals promiscuous exchange of mimicry adaptations among species. *Nature* **487**, 94–98 (2012).
12. S. Lamichhaney *et al.*, Evolution of Darwin's finches and their beaks revealed by genome sequencing. *Nature* **518**, 371–375 (2015).

13. E. J. Richards, M. R. Servedio, C. H. Martin, Searching for sympatric speciation in the genomic era. *BioEssays* **41**, e1900047 (2019).
14. J. I. Meier *et al*., Hybridization explains rapid adaptive radiation in Lake Mweru cichlid fishes. *Nat. Commun.* **10**, 5391 (2019).
15. J. Diamond, Evolution of ecological segregation in the New Guinea montane avifauna. *Community Ecol.*, 98–125 (1986).
16. T. J. Streelman, P. D. Danley, The stages of vertebrate evolutionary radiation. *Trends Ecol. Evol.* **18**, 126–131 (2003).
17. J. B. Losos, P. H. Harvey, A. J. Leigh Brown, J. M. Smith, Community evolution in greater Antillean Anolis lizards: Phylogenetic patterns and experimental tests. *Philos. Trans. R. Soc. Lond. B Biol. Sci.* **349**, 69–75 (1995).
18. J. T. Streelman, M. Alfaro, M. W. Westneat, D. R. Bellwood, S. A. Karl, Evolutionary history of the parrotfishes: Biogeography, ecomorphology, and comparative diversity. *Evolution* **56**, 961–971 (2002).
19. P. D. Danley, T. D. Kocher, Speciation in rapidly diverging systems: Lessons from Lake Malawi. *Mol. Ecol.* **10**, 1075–1086 (2001).
20. F. Ronco *et al*., Drivers and dynamics of a massive adaptive radiation in cichlid fishes. *Nature* **589**, 76–81 (2021).
21. R. Lande, Models of speciation by sexual selection on polygenic traits. *Proc. Natl. Acad. Sci. U.S.A.* **78**, 3721–3725 (1981).
22. E. Mayr, *Animal Species and Evolution* (Belknap, Cambridge, MA, 1963).
23. R. B. Huey, P. E. Hertz, B. Sinervo, Behavioral drive versus behavioral inertia in evolution: A null model approach. *Am. Nat.* **161**, 357–366 (2003).
24. J. B. Losos, T. W. Schoener, D. A. Spiller, Predator-induced behaviour shifts and natural selection in field-experimental lizard populations. *Nature* **432**, 505–508 (2004).
25. L. C. Sallan, M. Friedman, Heads or tails: Staged diversification in vertebrate evolutionary radiations. *Proc. Biol. Sci.* **279**, 2025–2032 (2012).
26. R. E. Glor, Phylogenetic insights on adaptive radiation. *Annu. Rev. Ecol. Evol. Syst.* **41**, 251–270 (2010).
27. S. Duchêne, R. Lanfear, Phylogenetic uncertainty can bias the number of evolutionary transitions estimated from ancestral state reconstruction methods. *J. Exp. Zoolog. B Mol. Dev. Evol.* **324**, 517–524 (2015).
28. Z. D. Blount, A case study in evolutionary contingency. *Stud Hist Philos Biol Biomed Sci* **58**, 82–92 (2016).
29. Z. D. Blount, R. E. Lenski, J. B. Losos, Contingency and determinism in evolution: Replaying life's tape. *Science* **362**, eaam5979 (2018).
30. Z. D. Blount, C. Z. Borland, R. E. Lenski, Historical contingency and the evolution of a key innovation in an experimental population of *Escherichia coli*. *Proc. Natl. Acad. Sci. U.S.A.* **105**, 7899–7906 (2008).
31. Z. D. Blount, J. E. Barrick, C. J. Davidson, R. E. Lenski, Genomic analysis of a key innovation in an experimental *Escherichia coli* population. *Nature* **489**, 513–518 (2012).
32. D. M. Weinreich, N. F. Delaney, M. A. DePristo, D. L. Hartl, Darwinian evolution can follow only very few mutational paths to fitter proteins. *Science* **312**, 111–114 (2006).
33. J. D. Fry, Mechanisms of naturally evolved ethanol resistance in Drosophila melanogaster. *J. Exp. Biol.* **217**, 3996–4003 (2014).
34. R. D. Tarvin *et al*., Interacting amino acid replacements allow poison frogs to evolve epibatidine resistance. *Science* **357**, 1261–1266 (2017).
35. M. Karageorgi *et al*., Genome editing retraces the evolution of toxin resistance in the monarch butterfly. *Nature* **574**, 409–412 (2019).
36. S. E. Miller *et al*., Evolutionary dynamics of recent selection on cognitive abilities. *Proc. Natl. Acad. Sci. U.S.A.* **117**, 3045–3052 (2020).
37. S. Nakagome *et al*., Estimating the ages of selection signals from different epochs in human history. *Mol. Biol. Evol.* **33**, 657–669 (2016).
38. J. Smith, G. Coop, M. Stephens, J. Novembre, Estimating time to the common ancestor for a beneficial allele. *Mol. Biol. Evol.* **35**, 1003–1017 (2018).
39. M. E. S. John, K. E. Dixon, C. H. Martin, Oral shelling within an adaptive radiation of pupfishes: Testing the adaptive function of a novel nasal protrusion and behavioural preference. *J. Fish Biol.* **97**, 163–171 (2020).
40. C. H. Martin, P. C. Wainwright, A remarkable species flock of Cyprinodon pupfishes endemic to San Salvador Island, Bahamas. *Bull. Peabody Mus. Nat. Hist.* **54**, 231–241 (2013).
41. M. E. St John, R. Holzman, C. H. Martin, Rapid adaptive evolution of scale-eating kinematics to a novel ecological niche. *J. Exp. Biol.* **223**, jeb217570 (2020).
42. C. H. Martin, Context dependence in complex adaptive landscapes: Frequency and trait-dependent selection surfaces within an adaptive radiation of caribbean pupfishes. *Evolution* **70**, 1265–1282 (2016).
43. C. H. Martin, P. C. Wainwright, Multiple fitness peaks on the adaptive landscape drive adaptive radiation in the wild. *Science* **339**, 208–211 (2013).
44. C. H. Martin, K. J. Gould, Surprising spatiotemporal stability of a multi-peak fitness landscape revealed by independent field experiments measuring hybrid fitness. *Evol. Lett.* **4**, 530–544 (2020).
45. C. H. Martin, P. C. Wainwright, Trophic novelty is linked to exceptional rates of morphological diversification in two adaptive radiations of Cyprinodon pupfish. *Evolution* **65**, 2197–2212 (2011).
46. M. E. St John, J. A. McGirr, C. H. Martin, The behavioral origins of novelty: Did increased aggression lead to scale-eating in pupfishes? *Behav. Ecol.* **30**, 557–569 (2019).
47. J. A. McGirr, C. H. Martin, Parallel evolution of gene expression between trophic specialists despite divergent genotypes and morphologies. *Evol. Lett.* **2**, 62–75 (2018).
48. D. Bryant, R. Bouckaert, J. Felsenstein, N. A. Rosenberg, A. RoyChoudhury, Inferring species trees directly from biallelic genetic markers: Bypassing gene trees in a full coalescent analysis. *Mol. Biol. Evol.* **29**, 1917–1932 (2012).
49. R. R. Bouckaert, DensiTree: Making sense of sets of phylogenetic trees. *Bioinformatics* **26**, 1372–1373 (2010).
50. S. Schiffels, R. Durbin, Inferring human population size and separation history from multiple genome sequences. *Nat. Genet.* **46**, 919–925 (2014).
51. F. M. Hagey, J. Mylroie, Pleistocene lake and lagoon deposits, San Salvador Island, Bahamas. *Geol. Soc. Am.* **30**, 77–90 (1995).
52. B. J. Turner, D. D. Duvernell, T. M. Bunt, M. G. Barton, Reproductive isolation among endemic pupfishes (Cyprinodon) on San Salvador Island, Bahamas: Microsatellite evidence. *Biol. J. Linn. Soc. Lond.* **95**, 566–582 (2008).
53. P. U. Clark *et al*., The last glacial maximum. *Science* **325**, 710–714 (2009).
54. D. H. Alexander, J. Novembre, K. Lange, Fast model-based estimation of ancestry in unrelated individuals. *Genome Res.* **19**, 1655–1664 (2009).
55. P. Pavlidis, D. Živkovic, A. Stamatakis, N. Alachiotis, SweeD: Likelihood-based detection of selective sweeps in thousands of genomes. *Mol. Biol. Evol.* **30**, 2224–2234 (2013).
56. N. Alachiotis, A. Stamatakis, P. Pavlidis, OmegaPlus: A scalable tool for rapid detection of selective sweeps in whole-genome datasets. *Bioinformatics* **28**, 2274–2275 (2012).
57. A. A. Echelle, E. W. Carson, A. F. Echelle, D. Bussche, T. E. Dowling, Historical biogeography of the new-World pupfish genus Cyprinodon (Teleostei: Cyprinodontidae). *Copeia* **2005**, 320–339 (2005).
58. T. Mendes Maia, D. Gogendeau, C. Pennetier, C. Janke, R. Basto, Bug22 influences cilium morphology and the post-translational modification of ciliary microtubules. *Biol. Open* **3**, 138–151 (2014).
59. Y. Takayanagi *et al*., Endogenous prolactin-releasing peptide regulates food intake in rodents. *J. Clin. Invest.* **118**, 4014–4024 (2008).
60. A. Suwa, M. Yoshino, C. Yamazaki, M. Naitou, R. Fujikawa, RMI1 deficiency in mice protects from diet and genetic-induced obesity. *FEBS J.* **277**, 677–686 (2010).
61. A. C. Choquette *et al*., Association between olfactory receptor genes, eating behavior traits and adiposity: Results from the Quebec family study. *Physiol. Behav.* **105**, 772–776 (2012).
62. M. Taye *et al*., Whole genome scan reveals the genetic signature of African Ankole cattle breed and potential for higher quality beef. *BMC Genet.* **18**, 11 (2017).
63. T. S. Hnasko, M. S. Szczypka, W. A. Alaynick, M. J. During, R. D. Palmiter, A role for dopamine in feeding responses produced by orexigenic agents. *Brain Res.* **1023**, 309–318 (2004).
64. E. A. Boyle, Y. I. Li, J. K. Pritchard, An expanded view of complex traits: From polygenic to omnigenic. *Cell* **169**, 1177–1186 (2017).
65. J. G. Crump, M. E. Swartz, C. B. Kimmel, An integrin-dependent role of pouch endoderm in hyoid cartilage development. *PLoS Biol.* **2**, E244 (2004).
66. K. LaMonica, H. L. Ding, K. B. Artinger, prdm1a functions upstream of itga5 in zebrafish craniofacial development. *Genesis* **53**, 270–277 (2015).
67. H. W. McGowan, J. A. Schuijers, B. L. Grills, S. J. McDonald, A. C. McDonald, Galnon, a galanin receptor agonist, improves intrinsic cortical bone tissue properties but exacerbates bone loss in an ovariectomised rat model. *J. Musculoskelet. Neuronal Interact.* **14**, 162–172 (2014).
68. C. H. Martin, P. A. Erickson, C. T. Miller, The genetic architecture of novel trophic specialists: Larger effect sizes are associated with exceptional oral jaw diversification in a pupfish adaptive radiation. *Mol. Ecol.* **26**, 624–638 (2017).
69. R. M. Green *et al*., Tfap2a-dependent changes in mouse facial morphology result in clefting that can be ameliorated by a reduction in Fgf8 gene dosage. *Dis. Model. Mech.* **8**, 31–43 (2015).
70. J. Zhang *et al*., Neural tube, skeletal and body wall defects in mice lacking transcription factor AP-2. *Nature* **381**, 238–241 (1996).
71. C. S. Teng *et al*., Altered bone growth dynamics prefigure craniosynostosis in a zebrafish model of Saethre-Chotzen syndrome. *eLife* **7**, 1–23 (2018).
72. S. Brewer, W. Feng, J. Huang, S. Sullivan, T. Williams, Wnt1-Cre-mediated deletion of AP-2α causes multiple neural crest-related defects. *Dev. Biol.* **267**, 135–152 (2004).
73. H. E. Seberg *et al*., TFAP2 paralogs regulate melanocyte differentiation in parallel with MITF. *PLoS Genet.* **13**, e100663 (2017).
74. M. T. J. Hague *et al*., Large-effect mutations generate trade-off between predatory and locomotor ability during arms race coevolution with deadly prey. *Evol. Lett.* **2**, 406–416 (2018).
75. R. T. Bronson, H. Sweet, C. A. Spencer, M. T. Davisson, Genetic and age related models of neurodegeneration in mice: Dystrophic axons. *J. Neurogenet.* **8**, 71–83 (1992).
76. H. J. McMillan *et al*., Recessive mutations in ATP8A2 cause severe hypotonia, cognitive impairment, hyperkinetic movement disorders and progressive optic atrophy. *Orphanet J. Rare Dis.* **13**, 86 (2018).
77. C. Mccormick *et al*., The putative tumour suppressor EXT1 alters the expression of cell-surface heparan sulfate. *Nat. Genet.* **19**, 158–161 (1998).
78. S. Sinha *et al*., Unsuspected osteochondroma-like outgrowths in the cranial base of Hereditary Multiple Exostoses patients and modeling and treatment with a BMP antagonist in mice. *Nat. Genet.* **13**, e1006742 (2017).
79. L. K. Marles, E. M. Peters, D. J. Tobin, N. A. Hibberts, K. U. Schallreuter, Tyrosine hydroxylase isoenzyme I is present in human melanosomes: A possible novel function in pigmentation. *Exp. Dermatol.* **12**, 61–70 (2003).
80. A. D'Osualdo, J. C. Reed, NLRP1, a regulator of innate immunity associated with vitiligo. *Pigment Cell Melanoma Res.* **25**, 5–8 (2012).
81. L. Qiao *et al*., Tyrosine Hydroxylase is crucial for maintaining pupal tanning and immunity in Anopheles sinensis. *Sci. Rep.* **6**, 29835 (2016).
82. M. Kirkpatrick, V. Ravigné, Speciation by natural and sexual selection: Models and experiments. *Am. Nat.* **159**, S22–S35 (2002).
83. D. I. Bolnick, B. M. Fitzpatrick, Sympatric speciation: Models and empirical evidence. *Annu. Rev. Ecol. Evol. Syst.* **38**, 459–487 (2007).

84. M. R. Servedio, J. W. Boughman, The role of sexual selection in local adaptation and speciation. *Annu. Rev. Ecol. Evol. Syst.* **48**, 85–109 (2017).
85. K. Laue, M. Jänicke, N. Plaster, C. Sonntag, M. Hammerschmidt, Restriction of retinoic acid activity by Cyp26b1 is required for proper timing and patterning of osteogenesis during zebrafish development. *Development* **3787**, 3775–3787 (2008).
86. K. M. Spoorendonk *et al*., Retinoic acid and Cyp26b1 are critical regulators of osteogenesis in the axial skeleton. *Development* **3774**, 3765–3774 (2008).
87. E. B. Rosenblum *et al*., Goldilocks meets santa Rosalia: An ephemeral speciation model explains patterns of diversification across time scales. *Evol. Biol.* **39**, 255–261 (2012).
88. C. H. Martin, E. J. Richards, The paradox behind the pattern of rapid adaptive radiation: How can the speciation process sustain itself through an early burst? *Annu. Rev. Ecol. Evol. Syst.* **50**, 569–593 (2019).
89. A. A. Comeault, D. R. Matute, Genetic divergence and the number of hybridizing species affect the path to homoploid hybrid speciation. *Proc. Natl. Acad. Sci. U.S.A.* **115**, 9761–9766 (2018).
90. R. G. Gillespie *et al*., Comparing adaptive radiations across space, time, and taxa. *J. Hered.* **111**, 1–20 (2020).
91. M. A. DePristo *et al*., A framework for variation discovery and genotyping using next-generation DNA sequencing data. *Nat. Genet.* **43**, 491–498 (2011).
92. S. Purcell *et al*., PLINK: A tool set for whole-genome association and population-based linkage analyses. *Am. J. Hum. Genet.* **81**, 559–575 (2007).
93. S. X. Ge, D. Jung, ShinyGO: A graphical enrichment tool for animals and plants. *Bioinformatics* **36**, 2628–2629 (2020).
94. X. Zhou, P. Carbonetto, M. Stephens, Polygenic modeling with bayesian sparse linear mixed models. *PLoS Genet.* **9**, e1003264 (2013).
95. J. K. Pritchard, J. K. Pickrell, G. Coop, The genetics of human adaptation: Hard sweeps, soft sweeps, and polygenic adaptation. *Curr. Biol.* **20**, R208–R215 (2010).
96. S. H. Martin, J. W. Davey, C. D. Jiggins, Evaluating the use of ABBA-BABA statistics to locate introgressed loci. *Mol. Biol. Evol.* **32**, 244–257 (2015).
97. R. Tournebize, V. Poncet, M. Jakobsson, Y. Vigouroux, S. Manel, McSwan: A joint site frequency spectrum method to detect and date selective sweeps across multiple population genomes. *Mol. Ecol. Resour.* **19**, 283–295 (2019).
98. E. J. Richards, Adaptive radiation of Caribbean pupfish is assembled from an ancient and disparate spatiotemporal landscape. National Center for Biotechnology Information. https://www.ncbi.nlm.nih.gov/bioproject/PRJNA690558. Deposited 7 January 2021.
99. E. J. Richards, Adaptive introgression contributes to microendemic radiation of Caribbean pupfishes. National Center for Biotechnology Information. https://www.ncbi.nlm.nih.gov/bioproject/PRJNA394148. Deposited 13 July 2017.
100. J. A. McGirr, Craniofacial divergence in Caribbean Pupfishes. National Center for Biotechnology Information. https://www.ncbi.nlm.nih.gov/bioproject/PRJNA391309. Deposited 21 June 2017.
101. J. A. McGirr, RNAseq of Cyprinodon pupfishes. National Center for Biotechnology Information. https://www.ncbi.nlm.nih.gov/bioproject/PRJNA305422. Deposited 8 December 2015.
102. C. H. Martin, Cyprinodon brontotheroides isolate:CRPMF4-2017. National Center for Biotechnology Information. https://www.ncbi.nlm.nih.gov/bioproject/PRJNA685538. Deposited 15 December 2020.
103. E. J. Richards, Data from: A vertebrate adaptive radiation is assembled from an ancient and disjunct spatiotemporal landscape. *Dryad Digital Repository*. https://doi.org/10.6078/D1C12S. Deposited 1 May 2021.
104. J. A. McGirr, Gene expression analyses code. GitHub. https://github.com/joemcgirr/fishfASE. Deposited 15 January 2019.
105. E. J. Richards. Spatiotemporal landscape of Caribbean pupfish analyses code. https://github.com/emiliejrichards/Spatiotemporal-Landscape-Caribbean-Pupfish. Deposited 1 May 2021.